Epigenomics

ISSN: (Print) (Online) Journal homepage: www.tandfonline.com/journals/iepi20

Combined therapy targeting AR and EZH2 curbs castration-resistant prostate cancer enhancing anti-tumor T-cell response

Irene Fischetti, Laura Botti, Roberta Sulsenti, Valeria Cancila, Claudia Enriquez, Renata Ferri, Marco Bregni, Filippo Crivelli, Claudio Tripodo, Mario P. Colombo & Elena Jachetti

To cite this article: Irene Fischetti, Laura Botti, Roberta Sulsenti, Valeria Cancila, Claudia Enriquez, Renata Ferri, Marco Bregni, Filippo Crivelli, Claudio Tripodo, Mario P. Colombo & Elena Jachetti (2024) Combined therapy targeting AR and EZH2 curbs castration-resistant prostate cancer enhancing anti-tumor T-cell response, Epigenomics, 16:9, 653-670, DOI: 10.2217/epi-2023-0374

To link to this article: https://doi.org/10.2217/epi-2023-0374

© 2024 The Authors

View supplementary material

Published online: 26 Mar 2024.

Submit your article to this journal

Article views: 879

View related articles

View Crossmark data

Full Terms & Conditions of access and use can be found at
https://www.tandfonline.com/action/journalInformation?journalCode=iepi20

Research Article

Epigenomics

Combined therapy targeting AR and EZH2 curbs castration-resistant prostate cancer enhancing anti-tumor T-cell response

Irene Fischetti[1], Laura Botti[1], Roberta Sulsenti[1], Valeria Cancila[2], Claudia Enriquez[§,1], Renata Ferri[1], Marco Bregni[3], Filippo Crivelli[4], Claudio Tripodo[2], Mario P. Colombo[‡,1] & Elena Jachetti*[,‡,1]

[1]Molecular Immunology Unit, Department of Experimental Oncology, Fondazione IRCCS Istituto Nazionale dei Tumori di Milano, Milan, Italy

[2]Tumor Immunology Unit, Department of Health Sciences, University of Palermo, Italy

[3]ASST Valle Olona, Busto Arsizio, Italy

[4]Anatomia Patologica, ASST Valle Olona, Busto Arsizio, Italy

*Author for correspondence: Tel.: +39 022 390 3232; elena.jachetti@istitutotumori.mi.it

[‡]Co-last authors

[§]Current address: Lymphoid Organ Development Unit, Division of Experimental Oncology, IRCCS San Raffaele Scientific Institute, Milan, Italy

Aim: Castration-resistant prostate cancer (CRPC) eventually becomes resistant to androgen receptor pathway inhibitors like enzalutamide. Immunotherapy also fails in CRPC. We propose a new approach to simultaneously revert enzalutamide resistance and rewire anti-tumor immunity. **Methods:** We investigated *in vitro* and in subcutaneous and spontaneous mouse models the effects of combining enzalutamide and GSK-126, a drug inhibiting the epigenetic modulator EZH2. **Results:** Enzalutamide and GSK-126 synergized to reduce CRPC growth, also restraining tumor neuroendocrine differentiation. The anti-tumor activity was lost in immunodeficient mice. Indeed, the combination treatment awoke cytotoxic activity and IFN-γ production of tumor-specific $CD8^+$ T lymphocytes. **Conclusion:** These results promote the combination of enzalutamide and GSK-126 in CRPC, also offering new avenues for immunotherapy in prostate cancer.

Plain language summary: Prostate cancer depends on hormones called androgens for its growth. Therefore, hormonal therapies are commonly used. However, the tumor often does not respond to these treatments and new therapeutic approaches are needed. Here, using cell and mouse models, we have tested a new combination between hormone therapy and a drug that restrains an enzyme regulating gene expression. Our results have shown that this combination therapy not only reduces the growth of the tumor but also stops it from becoming more aggressive. This is really important because aggressive prostate cancer is much harder to treat. We have also found that this approach helps the immune system recognizing and attacking cancer cells. More research is needed to identify the mechanism of action of this treatment. However, our findings suggest that this approach could pave the way for new therapeutic strategies, including using immunotherapy, typically unsuccessful in treating prostate cancer.

Tweetable abstract: Castration-resistant prostate cancer is a fatal disease in which immunotherapy failed. Combined therapy inhibiting the androgen receptor and the epigenetic regulator EZH2 can revert castration resistance and promote anti-tumor immunity.

First draft submitted: 25 October 2023; Accepted for publication: 7 March 2024; Published online: 26 March 2024

Keywords: castration resistance • epigenetic regulation • mouse models • prostate cancer • tumor immunology

Taylor & Francis
Taylor & Francis Group

Graphical abstract:

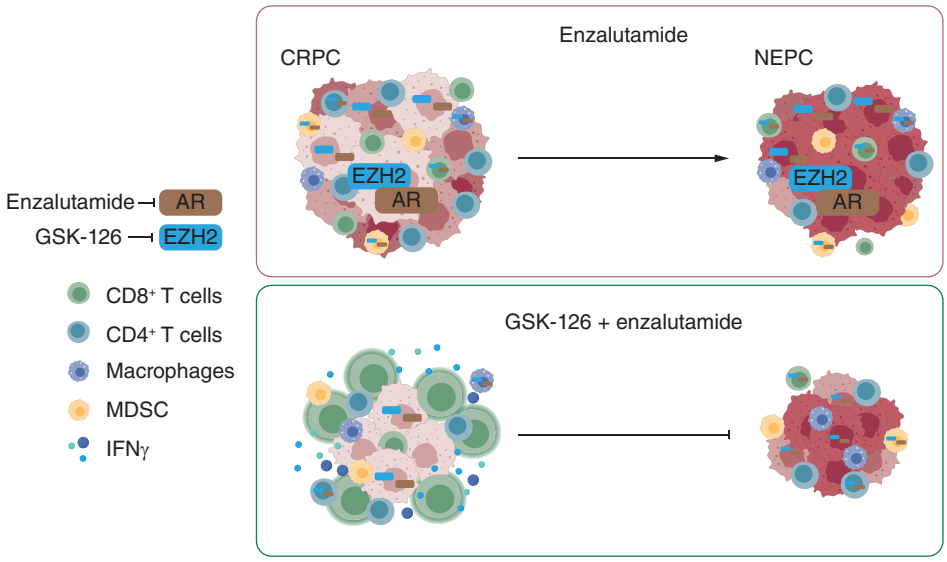

Prostate cancer ranks among the top causes of cancer-related mortality globally [1]. Advanced/metastatic tumors subjected to androgen-deprivation therapy (ADT) ultimately progress to become castration resistant (castration-resistant prostate cancer [CRPC]). Despite availability of novel androgen receptor pathway inhibitors (ARPIs), such as enzalutamide, prognosis of CRPC remains poor. Resistance to ADT/ARPI is linked to cellular plasticity [2] and the development of aggressive, fatal, neuroendocrine prostate cancer (NEPC), which counts for about 20–30% of patients who bypass hormone therapies [3,4]. *De novo* NEPC can also occur, albeit rarely (<1% of patients at first diagnosis). Thus, effective therapies for CRPC and NEPC are needed [5].

Immune checkpoint blockade is now the mainstream option for several solid tumors, but unsuccessful in prostate cancer [6]. Indeed, despite its potential immunogenicity [7], prostate cancer is a 'cold' tumor, with few infiltrating effector T cells and an immunosuppressive microenvironment governed by myeloid-derived suppressor cells (MDSCs) [8,9] and regulatory T cells (Treg) [10], also further recruited following ADT [10,11]. Notably, immune cells have the androgen receptor (AR) [12], and AR signaling can contribute to immunosuppression [13] directly transcribing *Foxp3* in Treg cells [14], and blunting effector functions in T cells [15]. AR signaling can also promote M2 polarization of macrophages [16], production of IL-10 and TGF by neutrophils [17], and either foster or inhibit MDSC recruitment [18,19]. Therefore, treatment with ADT/ARPI could potentially reshape the tumor microenvironment.

A second approach to mold the immune system could rely on epigenetic reprogramming. Enhancer of zeste homolog 2 (EZH2) is the catalytic subunit of the polycomb repressive complex 2, a transcriptional repressor [20]. In several preclinical tumor models EZH2 genetic or pharmacologic inhibition induced recruitment and cytokine production of effector T cells, and skewed Treg toward pro-inflammatory functions [21–23]. Moreover, a few studies show either tumor MDSC recruitment [24] or inhibition [25] upon EZH2 targeting. Similarly, it was shown that EZH2 inhibition holds the potential to skew macrophage polarization [26,27].

EZH2 also regulates cellular differentiation and malignant proliferation [28], and phase I/II trials are currently assessing the activity of EZH2 inhibitors in patients with solid tumors [29]. In prostate cancer, EZH2 is a marker of aggressive and metastatic disease [30], known to contribute to cell invasiveness through repression of E-cadherin expression [31]. Furthermore, the expression of a polycomb related signature has been associated with poor outcome in patients [32]. EZH2 can also directly promote the expression of AR, in a polycomb independent manner [33,34]. Finally, it has been found that EZH2 is upregulated in CRPC and involved in NEPC differentiation [35,36]. These data highlight the therapeutic potential of EZH2 inhibitors in prostate cancer. Indeed the concomitant treatment with enzalutamide and EZH2 inhibitors restrained CRPC/NEPC growth in different preclinical models [37,38].

Therefore, in prostate cancer the combination of ADT/ARPI and EZH2 inhibitors could exert a dual effect: restoring hormone sensitivity of tumor cells and awakening the antitumor immune response. This new hypothesis is herein investigated by exploiting in preclinical models, *in vitro* and *in vivo*.

Taylor & Francis
Taylor & Francis Group

Materials & methods

Cell lines

T1525, T23 and ST4787 murine prostate cancer cells were characterized previously [39,40]. All murine cells were cultured in DMEM (Gibco) supplemented with 10% of fetal bovine serum (FBS; Gibco), 200 U/ml penicillin (Cambrex), 150 U/ml streptomycin, 10 mmol/l Hepes, 10 mmol/l sodium pyruvate (Gibco), and 2 mmol/l L-glutamine. LNCaP, 22RV1 and PC3 human prostate cancer cells were purchased from ATCC (cat. no: CRL-1740, CRL-2505D, CRL-1435). Cells were tested for Mycoplasma as in [40]. Human cells were cultured in RPMI-1640 (Gibco) supplemented with 10% of FBS, 200 U/m penicillin, 150 U/ml streptomycin, 10 mM sodium pyruvate, and 2 mM L-glutamine; for LNCaP and 22Rv1 cells, a 2.5 g/l of D-(+)-glucose (Sigma Aldrich) were also added to the culture media. For proliferation experiments, 3.5×10^4 cells were seeded in 6-well plates, and the following day treated with enzalutamide (Selleckchem S1250; 5, 10, 12.5 or 25 μM, as indicated in each experiment), GSK-126 (Selleckchem S7061; 1, 2.5, or 5 μM, as indicated in each experiment) or their combination (hereafter named COMBO). Cell count was evaluated after 96 h with the XTT assay kit (Applichem) or by trypan blue evaluation. For the evaluation of H3K27me3 expression, cells were cultured in 6-well plates, either treated or not with GSK-126 (5 μM) for 96 h, and then lysed for western blot analysis. For evaluation of cytokine production, murine cell lines were seeded in 12-well plates and the following day were either left untreated or treated with enzalutamide (10 μM), GSK-126 (5 μM), or COMBO. Cytokine production was evaluated after 24, 48 and 96 h by flow cytometry.

Mice & treatments

C57BL/6 and NSG male mice were purchased from Charles River Laboratories. 2×10^6 T23 or 1×10^6 ST4787 cells were subcutaneously injected in saline solution. When tumor volume reached 40–50 mm^3, mice were treated with mock solution (DMSO and cremophor in saline solution), enzalutamide (30 mg/kg), GSK-126 (30 mg/Kg) or COMBO, intraperitoneally (i.p.) 3 days per week, for 2 weeks. Mice were sacrificed the day after the last treatment.

TRAMP mice on C57BL6/J background [C57BL/6-tgN (TRAMP)8247Ng] [41] were maintained as in [42]. For therapy experiments, 20 weeks old TRAMP mice underwent surgical castration as described in [40,42]. Starting from 3 weeks post-castration mice were treated with mock solution, enzalutamide, GSK-126 or COMBO, ip., once per week, and then sacrificed at 35 weeks of age. For cytotoxicity experiments, 16 weeks-old TRAMP mice were treated i.p. twice per week, for 3 weeks.

Animal housing and experimentation were performed following institutional guidelines and the Italian law (D.Lgs. 26/2014). *In vivo* experiments were approved by the Italian Ministry of Health (authorization number 8/2020-PR).

Antibodies

All the antibodies used in this study are listed in Supplementary Table 1.

Western blot

For AR and EZH2 evaluation, cells were lysed in RIPA buffer containing protease and phosphatase inhibitors. For H3K27me3 evaluation, cells were lysed in a buffer containing 0.5 M TrisHCl (pH 6.8) and 5% SDS plus protease and phosphatase inhibitors. Lysates were boiled for 5 min and then sonicated for 20 s at 25 A. Lysates were quantified (we used the Pierce BCA Protein assay kit catalog no. 23225 Thermo Scientific for RIPA samples and the Euroclone Quantum Micro Protein kit catalog no. EMP015480 for SDS samples), run on NuPAGE Bis-Tris gels (4–12%) and transferred on a nitrocellulose membrane. Membranes were blocked 1 h at room temperature with 5% BSA in PBS- 0.5% tween and then incubated overnight at 4° with primary antibody. HRP conjugated secondary antibody was then incubated 1 h at room temperature. Staining was revealed with ECL solution and images were acquired on an x-ray film or with Azure 600 imager (AZI600-0, Azure Biosystems). Blots were quantified with the ImageJ software.

Classification of tumor lesions in TRAMP mice

Murine urogenital apparata were fixed in formalin and embedded in paraffin (FFPE). Sections (5 μm) were deparaffined and rehydrated, stained with H&E (BioOptica) and evaluated by a pathologist. In serial sections, immunofluorescence for luminal (CK8) and neuroendocrine (SYP) markers was performed (see section 2.7).

Table 1. Patients' characteristics and EZH2 staining score.

Patient ID	Gleason score	EZH2 staining score
3	3+2	-
4	3+2	-
6	3+3	+/-
24	3+3	-
25	3+3	-
34	3+3	-
35	3+3	-
37	3+3	-
1	4+3	+/-
2	4+3	+/-
5	3+4	+
7	3+4	-
8	4+3	+
9	4+4	+
10	3+4	-
13	3+4	+
14	3+3	-
15	3+3	-
16	3+3	+/-
20	4+3	-
21	3+4	+
26	4+3	+
28	4+3	+
29	3+4	-
30	4+3	+
36	4+3	+/-
38	3+4	+
11	4+5	+/-
12	4+5	++
17	5+4	+/-
18	4+5	+++
19	5+4 focal neuroendocrine prostate cancer	+++
22	4+4	+++
23	5+4	+++
27	4+4	+/-
31	5+4	+
32	5+4	+++
33	4+5	++

The score index was assigned to distinguish intensity of EZH2 staining. - means no staining; +++ means maximum intensity.

Murine prostate lesions were scored according to histopathological and immunophenotypical analyses as described in [40] and in the Results section.

Human prostate cancer samples

FFPE prostatectomies from prostate cancer patients (n = 38) were obtained from ASST Valle Olona, Busto Arsizio (VA), Italy (Protocol number 0046679/18), upon informed consent and in accordance with the Helsinki Declaration. Tissue collection, fixation and processing followed standardized protocols as part of routine clinical activity. The Gleason Score of analyzed tumors is reported in Table 1.

Taylor & Francis
Taylor & Francis Group

Immunohistochemistry & immunofluorescence

FFPE tumor samples were cut in 5 µm sections, which were deparaffined and rehydrated. Antigen retrieval was performed utilizing the Novocastra Epitope Retrival Solution pH6 (Novocastra, Leica Biosystems), at 95°C for 15 min. Sections were brought to room temperature and washed with PBS. For immunohistochemistry, after neutralization of the endogenous peroxidase with 3% H2O2 and Fc blocking by a specific protein block (BSA 1%), the samples were incubated with the primary EZH2, AR or H3K23me3 antibodies overnight at 4° (antibodies are listed in Supplementary Table 1). Staining was revealed using a polymer detection kit (Novocastra, Leica Biosystems) or DAKO EnVison FLEX (Dako Omnis) as chromogenic substrate, followed by counterstaining with Harris hematoxylin (Novocastra, Leica Biosystems). Slides were acquired with a Leica DM4 B microscope equipped with a Leica DFC450 C digital camera, utilizing the LAS 4.8 software (Leica Biosystems). For double CK8/SYP staining, after antigen retrieval sections were blocked with PBS-Tween (0.1%) containing 5% of BSA. Primary conjugated antibodies were simultaneously incubated overnight at 4°C. Staining with DAPI (ThermoFisher Scientific) was performed for 10 min at room temperature. Slides were mounted with ProLong Diamond Antifade Mountant (ThermoFisher Scientific), and acquired with a Leica DM4 B microscope equipped with a Leica DFC450 C digital camera, utilizing the LAS X software (Leica Biosystems). Images were mounted and staining intensity were quantified using the ImageJ software. The EZH2 staining score on human tumor samples (Table 1) was determined in a blind fashion, comparing the staining intensity of all the slides, assigning (+++) to the maximum intensity observed and (-) to the lowest, and then re-assigning the values to all the slides.

RNA extraction & real-time PCR

T23 and ST4787 tumors were stored in RNA later (Thermofisher) at -80°C, and, when needed, were homogenized with TissueRuptor® (Qiagen) in RNA Lysis Buffer. For the isolation of $CD45^+$ cells, T23 tumors were instead digested with collagenase I (1 mg/ml Gibco™ by Life Technologies, catalog no. 17018-029) for 2 h at 37°C. Cell suspensions were then labeled with $CD45^+$ antibody and then sorted with a BD FACSMelody™ Cell Sorter. Dead cells were excluded by 7AAD staining.

Total RNA was extracted with Quick-RNA MicroPrep or MiniPrep kits (Zymo Research), quantified by Nanodrop 2000c spectrophotometer (ThermoFisher Scientific), and reverse transcribed using the High-Capacity cDNA Reverse Transcription Kit (TermoFisher Scientific, catalog no. 4368814). Real time-PCR was performed in a total volume of 20 µL using the Taqman® Fast Universal PCR Master Mix no Amperase UNG (ThermoFisher Scientific, catalog no. 4352042), 20 ng of cDNA, and Taqman probes for *Ar* (Mm00442688_m1), *Ezh2* (Mm00468464_m1) and *Gadph* (Mm99999915_g1). Values were normalized to internal control (*Gapdh*) and analyzed using the ΔCT method.

Flow cytometry

Cell suspensions were obtained from mechanical disgregation of murine spleens or from digestion of prostates and tumors with collagenase I (1 mg/ml) incubated 2 h at 37°C. For surface staining, cells were labeled 15 min at 4°C with the desired antibody mix. Fixable Viability Stain (BD Bioscience; cat. 565388) was added to exclude dead cells from the analysis. For intracellular cytokine detection, tumor or spleen derived cells were stimulated for 4 h with PMA/Ionomycin or with the Tag-$IV_{404\text{-}411}$ peptide (1 µg/ml), respectively, adding brefeldin A in the last 3 h. Cells were stained with surface markers and fixed with Foxp3/Transcription Factor Staining Buffer kit (Tonbo Biosciences, TNB-1022-L160 and TNB-1020-L050), respectively. Then, they were permeabilized (Perm buffer; TNB-1213-L150; Tonbo Biosciences) and stained with the desired intracellular antibody. Samples were acquired with BD LSRII Fortessa™ and analyzed with the Flow Jo software.

Immunization protocol & *in vivo* cytotoxicity assay

Dendritic cells (DCs) were prepared culturing bone marrow precursor isolated from the flushing of the tibias and femurs of a C57BL/6 mouse for 7 days in complete IMDM containing 10% of FBS, IL-4 (5 ng/ml; Peprotech) and GM-CSF (25 ng/ml; Peprotech). At day 7, DCs were stimulated for 7 h with LPS (1 µg/ml; Sigma), pulsed 1 hour with Tag-$IV_{404\text{-}411}$ peptide (2 µg/ml) and injected (2×10^5 DC/mouse) intradermal into the right flank of the mice. 6 days later mice were injected intravenously with 10^7 cells containing equal numbers of splenocytes labeled with either 1.25 µg/ml ($CFSE^{hi}$) or 0.125 µg/ml of CFSE ($CFSE^{low}$). $CFSE^{hi}$ cells were previously pulsed 1 h with Tag-$IV_{404\text{-}411}$ peptide. Mice were sacrificed the following day and spleens and prostates were collected and analyzed by flow cytometry for the evaluation of the presence of $CFSE^{hi}$ and $CFSE^{low}$ cells. Tag-specific cytolytic

activity was calculated as: (percentage $CFSE^{hi}$ cells) × 100/(percentage $CFSE^{low}$ cells), as in [9]. Spleen and prostates of mice were also analyzed by flow cytometry for immune infiltrate and cytokine production, as described above.

Magnetic beads purification & *in vitro* experiments

Splenocytes from C57BL/6 mice were stained with CD19 and CD11b APC-conjugated antibodies, labeled with anti-APC Microbeads (Miltenyi Biotec; 130-090-855) and loaded onto magnetic columns for T cell enrichment through negative selection. CFSE-labeled purified T cells were activated *in vitro* with anti-CD3 (2 μg/ml) and anti-CD28 (1 μg/ml), alone or with enzalutamide (10 μM), GSK-126 (5 μM) or COMBO. After 3 days, we tested proliferation (CFSE dilution) and IFN-γ production by flow cytometry.

Regulatory T cells were isolated from the spleen of naive TRAMP mice through the $CD4^+CD25^+$kit (Miltenyi; 130-091-041) and cultured *in vitro* overnight, alone or with enzalutamide, GSK-126 or COMBO. Cytokine production was evaluated through flow cytometry.

MDSC were isolated from the spleen of TRAMP mice treated *in vivo* with mock solution, enzalutamide, GSK-126 or COMBO. MDSC purification and suppressive assay were performed as described in [9].

Statistical analyses

We utilized the GraphPad Prism9 software. All experiments were performed at least two times. Pools of biological replicates obtained in all the independent experiments were performed and statistical analysis was run considering all the samples. Histograms report means ± SD of all biological replicates, which are represented by dots. Data were analyzed using two-way ANOVA for tumor growth comparison in subcutaneous models, the Fisher test for comparison of tumor frequency in castrated TRAMP mice and one-way ANOVA with *post hoc* Tukey's test for multiple comparisons for other experiments. *$p < 0.05$; **$p < 0.01$; ***$p < 0.001$, and ****$p < 0.0001$. Where p-value is not indicated, the comparison between groups is not statistically significant.

Results

A drug inhibiting EZH2 restores enzalutamide sensitivity in CRPC cells

For *in vitro* experiments, we utilized a panel of human prostate cancer cell lines, known to be either sensitive (LNCaP) or resistant (22Rv1, and PC3) to enzalutamide [44–46], and a panel of in-house generated murine prostate adenocarcinoma (T1525 and T23), and NEPC (ST4787) cells [39,40]. All the cells express AR and EZH2, except human PC3 cells that, as known [44], are AR negative (Figure 1A & B). Dose–response experiments showed that T1525 are sensitive to enzalutamide (IC50 10.86 μM), whereas both T23 and ST4787 are not (Figure 1C). We also performed dose–response experiments with the EZH2-inhibitor GSK-126 that, according to what previously shown in a different prostate cancer model [37], did not affect the proliferation of neither human nor murine prostate cancer cells (Figure 1D & E), despite effectively reducing histone H3 lysine 27 tri-methylation (H3K23me3), measured as readout of EZH2 methyltransferase activity (Figure 1F & G).

We then evaluated the effects of the combination of enzalutamide (10 μM) and GSK-126 (5 μM) against cell proliferation. In LNCaP and T1525 cells, only enzalutamide as single agent decreased cell proliferation but this effect was significantly increased by the combination of enzalutamide and GSK-126 (hereafter named COMBO; Figure 1H & I). Notably, the COMBO significantly reduced the proliferation of both T23 and 22Rv1 CRPC cells, which were insensitive to any of the two drugs given alone (Figure 1H & I). Neither PC3 nor ST4787 cells were affected by the treatments (Figure 1H & I). Therefore, inhibition of EZH2 can restore sensitivity to enzalutamide in both human and murine CRPC cells lines, but not in established NEPC cells.

Enzalutamide & GSK-126 combination restrains CRPC growth & NEPC differentiation *in vivo*

We then moved *in vivo*, subcutaneously injecting T23 or ST4787 cells in syngeneic C57BL/6 immunocompetent mice. Differently from *in vitro* experiments, in mice enzalutamide alone significantly reduced the growth of CRPC T23-derived tumors (Figure 2A), suggesting that the microenvironment could play a role in this effect. Tumors in the COMBO group were also significantly smaller than controls. Indeed, adding GSK-126 to enzalutamide seemed to further reduce tumor volumes, albeit the difference between the enzalutamide and the COMBO group was not statistically significant (Figure 2A). None of the treatments was effective in mice bearing ST4787 tumors (Figure 2B). Nevertheless, the concomitant treatment with GSK-126 inhibited NEPC differentiation of T23-derived tumors induced *in vivo* by enzalutamide (Figure 2C & Supplementary Figure 1A & B).

Taylor & Francis
Taylor & Francis Group

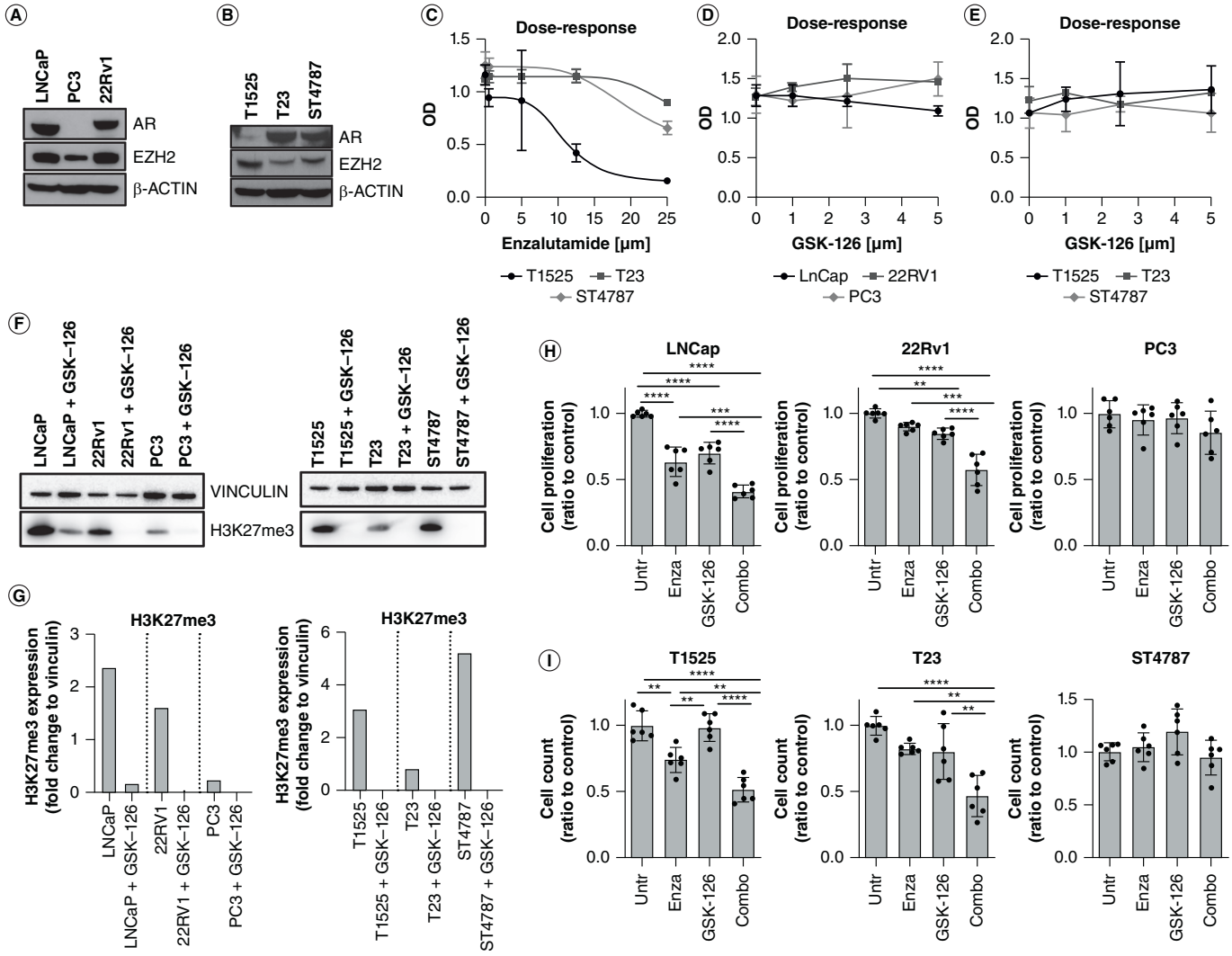

Figure 1. EZH2 inhibition restores enzalutamide sensitivity in castration-resistant prostate cancer cells. (A & B) Human (LNCaP, PC3, 22Rv1) and murine (T1525, T23, ST4787) prostate cancer cell lines were assessed for AR and EZH2 expression through western blot analysis. β-actin was used as housekeeping. **(C)** Murine cells were cultured with different doses of enzalutamide (0, 5, 12.5, and 25 μM) for 96 h and tested for proliferation by XTT assay. **(D & E)** Human and murine cells were cultured with different doses of GSK-126 (0, 1, 2.5, and 5 μM) for 96 h and tested for proliferation by XTT assay. **(F)** Human and murine cells were either left untreated or treated with GSK-126 (5 μM). After 96 h, H3K27me3 levels were tested by western blot. Vinculin was used as housekeeping. The western blot was repeated twice **(G)**. Quantification of F. **(H & I)** Human and murine cells were cultured in the presence of enzalutamide (10 μM), GSK-126 (5 μM), or their combination (Combo) as indicated, for 96 h and tested for proliferation through trypan blue cell counting. Histograms report mean ± SD of biological replicates (represented by dots), pooled from two independent experiments. One-way Anova followed by Tukey's multiple comparison test is used, $^{**}p < 0.01$; $^{***}p < 0.001$, and $^{****}p < 0.0001$. Where p-value is not indicated, the comparison between groups is not statistically significant.

To evaluate the therapeutic activity of enzalutamide and GSK-126 combination in a setting resembling a clinical situation where enzalutamide is administered after ADT, we then moved to the spontaneous TRAMP prostate cancer model, in which we can mimic ADT by surgical castration (Figure 2D & Supplementary Figure 1C & D). Results showed that castration caused tumor regression in 27% of mice, whereas the remaining 73% of castrated animals developed tumors scored as NEPC. The frequency of NEPC induced by castration was slightly reduced by administration of enzalutamide (54%) and not altered by GSK-126 (77%). Compared with castration only and to castration plus enzalutamide, the COMBO treatment respectively halved and reduced by a third the rate of NEPC (36% in castrated + COMBO vs 73% in castrated vs 54% in castrated + enzalutamide), significantly increasing the frequency of cured mice (55% of regression). Some CRPC were detected in the enzalutamide and COMBO

groups (8% and 9% respectively). Thus, the COMBO treatment can efficiently restrain NEPC differentiation in mouse models.

Antitumor effect of the COMBO treatment requires proficient immune response

To test whether immune cells contribute to the antitumor efficacy observed *in vivo*, we injected T23 cells in NSG mice, lacking lymphoid cells and having defective myeloid cells [47]. In these immunodeficient mice, the therapeutic effect of the enzalutamide alone and of the COMBO regimen was lost (Figure 2E). By immunohistochemistry, we checked that both the GSK-126 and the COMBO treatment reduced the levels of H3K23me3 in T23 tumors, both when grown in C57BL/6 and NSG mice, as well as in ST4787 tumors grown in C57BL/6 mice (Figure 3A). We also confirmed AR and EZH2 expression in tumor and stroma cells of T23 and ST4787-derived lesions by immunohistochemistry (Figure 3B). To best appreciate the expression of the two markers in tumor-infiltrating immune cells, we also performed a real time PCR to measure *Ar* and *Ezh2* transcript levels in RNA obtained from either whole murine tumors or FACS sorted infiltrating $CD45^+$ cells (Figure 3C). By immunohistochemistry, we also identified EZH2 positive tumor and stroma cells in high grade human prostate cancer (Figure 3D). Notably, EZH2 staining intensity was almost negative or dim in human tumors with low Gleason score, but increased in tumors with high Gleason score (4+5, 5+4) and NEPC features (Figure 3D & Table 1).

Results suggest that *in vivo* enzalutamide might rewire the immune microenvironment toward CRPC inhibition, an effect that could potentially be enhanced by concomitant administration of GSK-126. We therefore investigated by flow cytometry the immune milieu of T23 and ST4787 derived tumors (Figure 4 & Supplementary Figure 2). Total $CD45^+$ immune cells were higher in T23 samples. Among $CD45^+$ cells, in both tumor types $CD11b^+$ myeloid cells were predominant than $CD3^+$ lymphoid cells. $CD8^+$ T cells and $CD4^+$ Treg were prevalent in T23 and ST4787 tumors, respectively. Macrophages were the most representative cells in both tumor types, but skewed to M2 in ST4787 tumors. PMN- and M-MDSC equally infiltrated T23 and ST4787 samples. These results suggest that ST4787 NEPC tumors have a 'colder' microenvironment than T23 tumors. In both models none of the treatments altered the frequency of the immune cell population analyzed, neither in tumor (Figure 4) nor in spleen (Supplementary Figure 3), except for a slight increase of tumoral PMN-MDSC (Figure 4) and splenic M2 macrophages (Supplementary Figure 4), after both GSK-126 and COMBO treatment.

We therefore hypothesized that the antitumor effect seen in immunocompetent mice was related to differences in the function rather than in the frequency of immune cells.

Enzalutamide & GSK-126 COMBO enhances tumor-specific $CD8^+$ T cell activity *in vivo*

To dissect the activity of tumor-specific T cells we exploited TRAMP mice, where the SV40-Large T antigen (Tag) oncogene acts as a tumor-associated antigen, leading to persistent Tag-specific tolerance of $CD8^+$ T cells [9,48]. To test whether we could restore T cell functionality, we treated 16 weeks-old TRAMP mice with control mock solution, enzalutamide, GSK-126 or the COMBO. After 2 weeks, all mice were immunized with DCs pulsed with the CD8-immunodominant Tag_{IV} peptide [49] and killed one week later to test *in vivo* specific cytotoxic activity against Tag-expressing target cells, injected the day before (Figure 5A & Supplementary Figure 4). As known [9], *in vivo* Tag-specific $CD8^+$ T cell cytotoxic activity was very low in untreated TRAMP mice, but it significantly increased in TRAMP mice treated with the COMBO (Figure 5B). We also observed an increase of T cell cytotoxicity in the enzalutamide group, albeit not statistically significant. Furthermore, the effect was tumor specific, as the COMBO did not further increase T cell cytotoxicity in control wild type C57BL/6 mice, not tolerant against Tag (Figure 5B).

In the same cohorts, we tested frequency (Figure 5C) and cytokine production (Figure 5D) of prostate-infiltrating T cells. As experiments in the subcutaneous models (Figure 4) showed no modulation in the myeloid compartment, we spared macrophages from this analysis, but we still tested MDSC frequency, knowing from our previous studies that PMN-MDSC can restrain T cell activity in TRAMP mice [9]. None of the treatments altered immune cell recruitment (Figure 5C). However, the COMBO significantly increased IFN-γ production by $CD8^+$ T cells (Figure 5D), and IL-17 production by $CD4^+$ T cells (Figure 5D) in TRAMP mice. These changes were confined to the tumor microenvironment, as they were not detected in the spleen of TRAMP mice (Supplementary Figure 5) nor in the prostates of wild type, tumor free, C57BL/6 mice (Figure 5D).

These data indicate that the COMBO can increase the activity of tumor-specific T cells in prostate cancer.

Taylor & Francis
Taylor & Francis Group

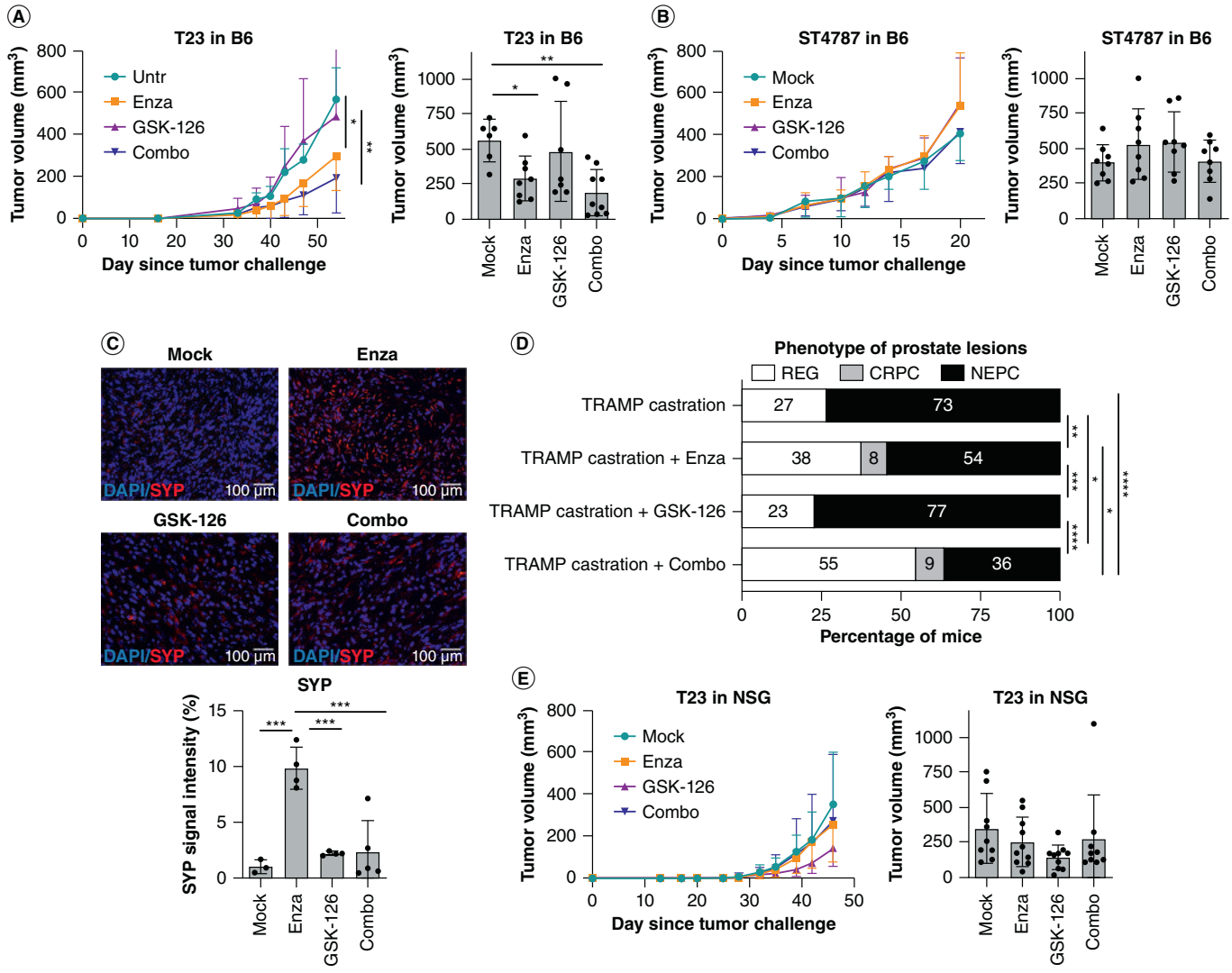

Figure 2. Antitumor effect of concomitant AR and EZH2 inhibition restrain castration-resistant prostate cancer and neuroendocrine prostate cancer *in vivo* and the effect is immune-dependent. (A & B) Tumor growth in C57BL/6 mice injected subcutaneously with T23 **(A)** or ST4787 **(B)** cells and treated with enzalutamide, GSK-126, or their combination (Combo). N = 8 mice for each group, pool of two independent experiments. Left graphs represent mean tumor volume; right histograms report mean tumor volume ± SD at the day of sacrifice, each dot is a mouse. Two-way Anova followed by Tukey's multiple comparison test: *$p < 0.05$. **(C)** SYP expression (red) was assessed in excised subcutaneous tumors of **(A)** by immunofluorescence. Blue staining is DAPI. Experiment was repeated two-times. SYP signal intensity was evaluated with ImageJ software. Histogram report mean ± SD, each dot is a mouse. One-way Anova followed by Tukey's multiple comparison test: ***$p < 0.001$. **(D)** TRAMP mice were surgically castrated at 20 weeks of age, and after 3 weeks either left untreated (n = 11) or treated with enzalutamide (n = 13), GSK-126 (n = 13), or their combination (Combo; [n = 11]) and sacrificed at 35 weeks of age. Histograms report the frequency of tumor lesions scored as neuroendocrine prostate cancer (NEPC), castration-resistant prostate cancer (CRPC) or regression (REG); numbers written in the bars indicate the relative percentages of each type of lesion. Murine prostate lesions were scored according to histopathological and immunophenotypical analyses (Supplementary Figure 1C & D) as follows: i) CRPC: lesions of high-grade prostatic intraepithelial neoplasia or adenocarcinoma characterized by CK8 positive atypical cells forming distorted/ill-defined glands within the stroma. ii) NEPC: composed of sheets and nests of medium-sized to large cells with high nuclear to cytoplasmic ratio and/or anaplastic morphology. Cells were immunoreactive for SYP and either negative (in case of pure small-cell NEPC) or positive for CK8 (in case of tumors with mixed adenocarcinoma and NEPC features, ref. [43]). When NEPC areas and CRPC or REG lesions were present in different lobes, the tumor was classified as NEPC. iii) Regression (REG): prostates with variable degree of glandular distortion characterized by dilated lumina with flattened or focally hyperplastic epithelia in the absence of overt nuclear atypia. Fisher test: *$p < 0.05$; **$p < 0.01$; ***$p < 0.001$, and ****$p < 0.0001$. **(E)** Tumor growth in immunodeficient NSG mice injected subcutaneously with T23 cells and treated with enzalutamide, GSK-126, or their combination (Combo). N = 8 mice for each group, pool of two independent experiments. Left graphs represent mean tumor volume; right histograms report mean tumor volume ± SD at the day of sacrifice, each dot is a mouse. Two-way Anova followed by Tukey's multiple comparison test was performed. In all graphs, where p-value is not indicated, the comparison between groups is not statistically significant.

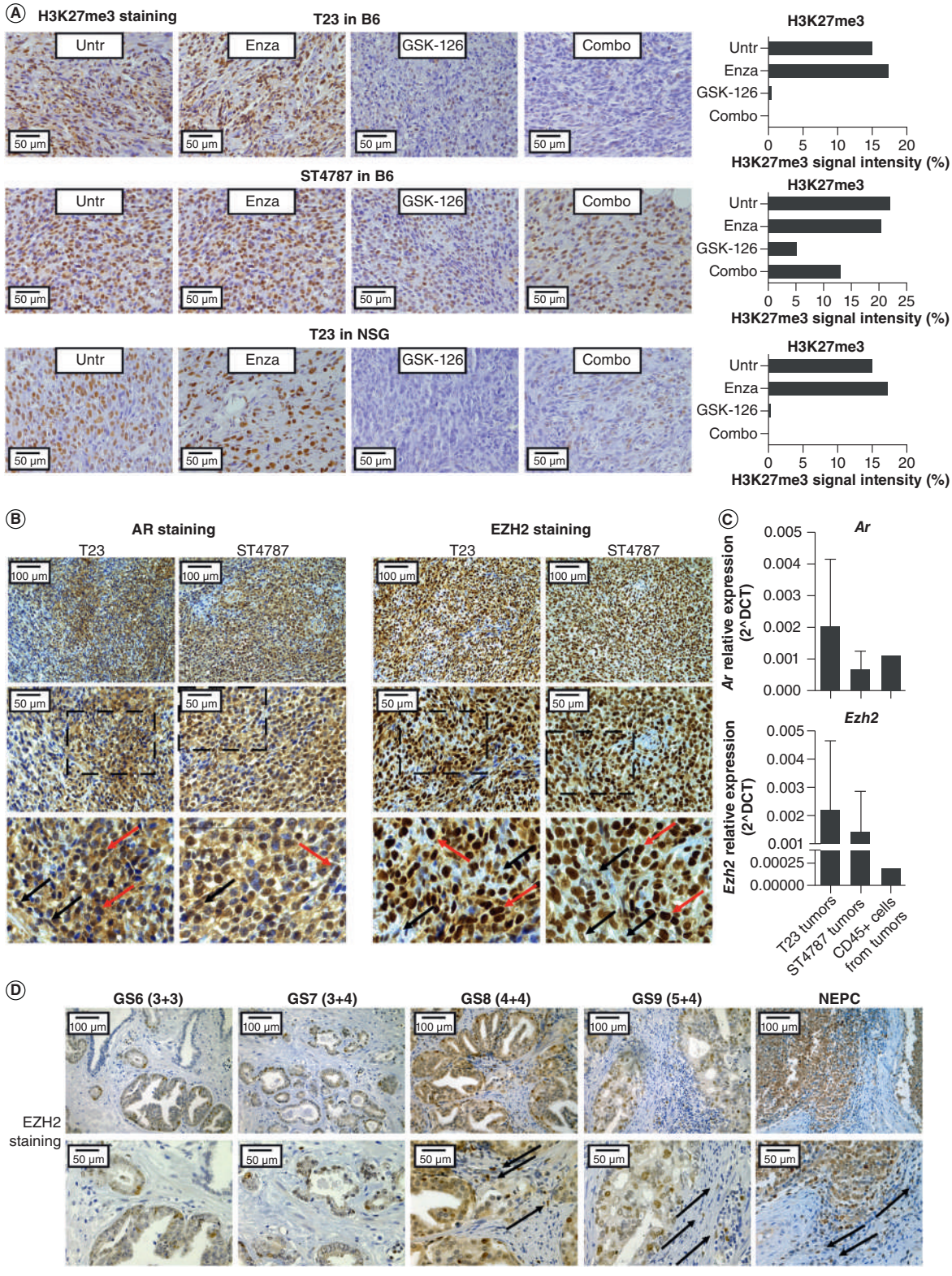

Figure 3. EZH2 is expressed in murine and human prostate cancer lesions. (A) Pictures show immunohistochemistry for H3K27me3 in T23 and ST4787 tumors collected from the experiments reported in Figure 2A, B and E. Histograms report staining intensity quantification, evaluated with ImageJ software. **(B)** Immunohistochemistry for AR and EZH2 on subcutaneously T23 and ST4787 lesions. Scale bars indicate magnifications. The lower panels are digital magnifications of selected areas indicated by a dotted line in the middle panels; red and black arrows indicate selected tumor and stromal cells, respectively **(C)**. Real time PCR for *Ar* and *Ezh2* on RNA samples collected from whole T23 and ST4787 tumors and from $CD45^+$ cells FACS sorted from T23 tumors (n = 2). **(D)** Immunohistochemistry for EZH2 on human prostate cancer lesions with different Gleason Score. Scale bars indicate magnifications. Black arrows indicate stromal cells.

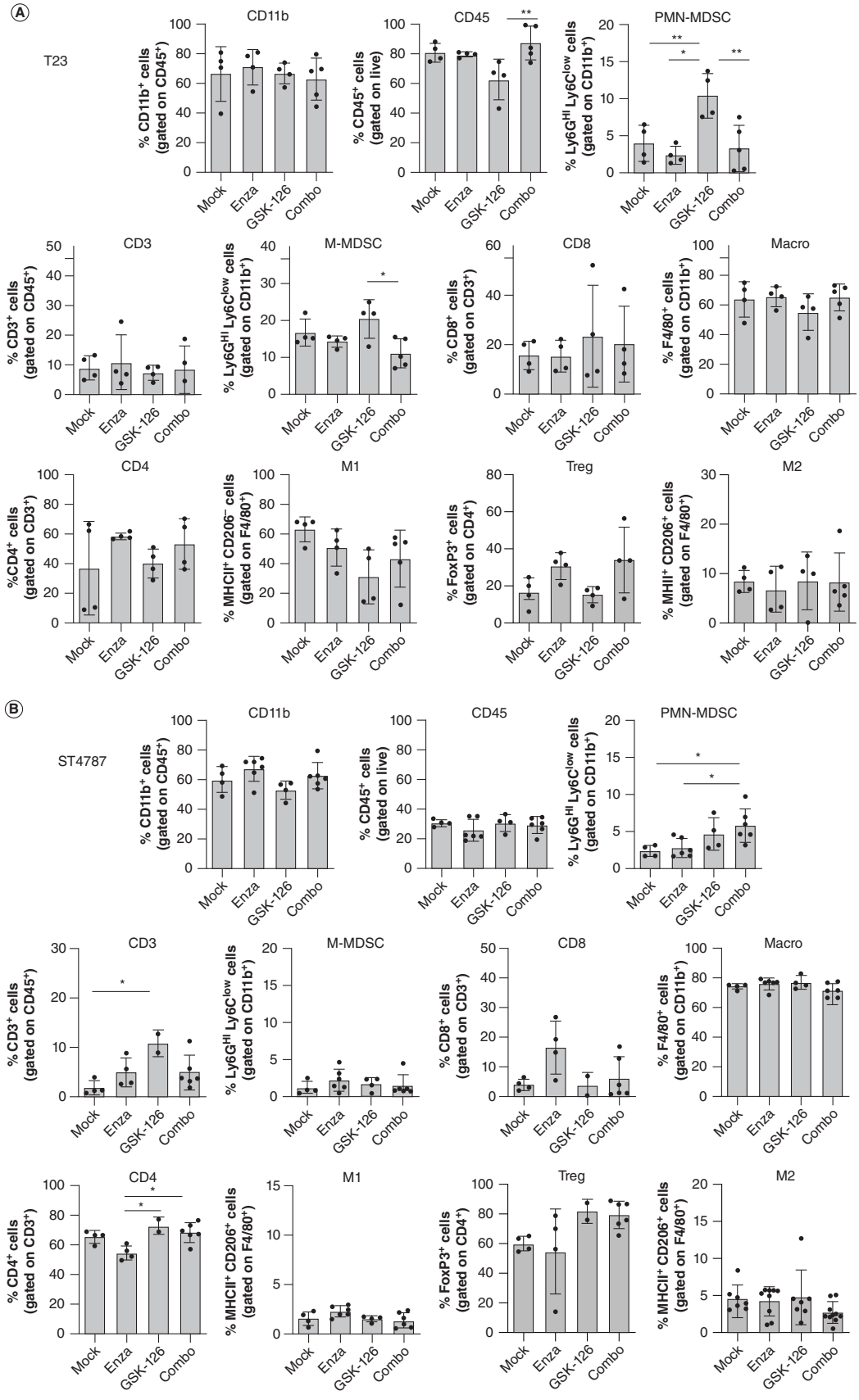

Figure 4. The COMBO treatment does not affect the frequency of immune subpopulations in subcutaneous tumors. Analysis of immune infiltrate of subcutaneous T23 **(A)** and ST4787 **(B)** tumors by flow cytometry. Histograms report mean ± SD, each dot is a mouse. One-way Anova followed by Tukey's multiple comparison test: *$p < 0.05$; **$p < 0.01$. Where p-value is not indicated, the comparison between groups is not statistically significant.

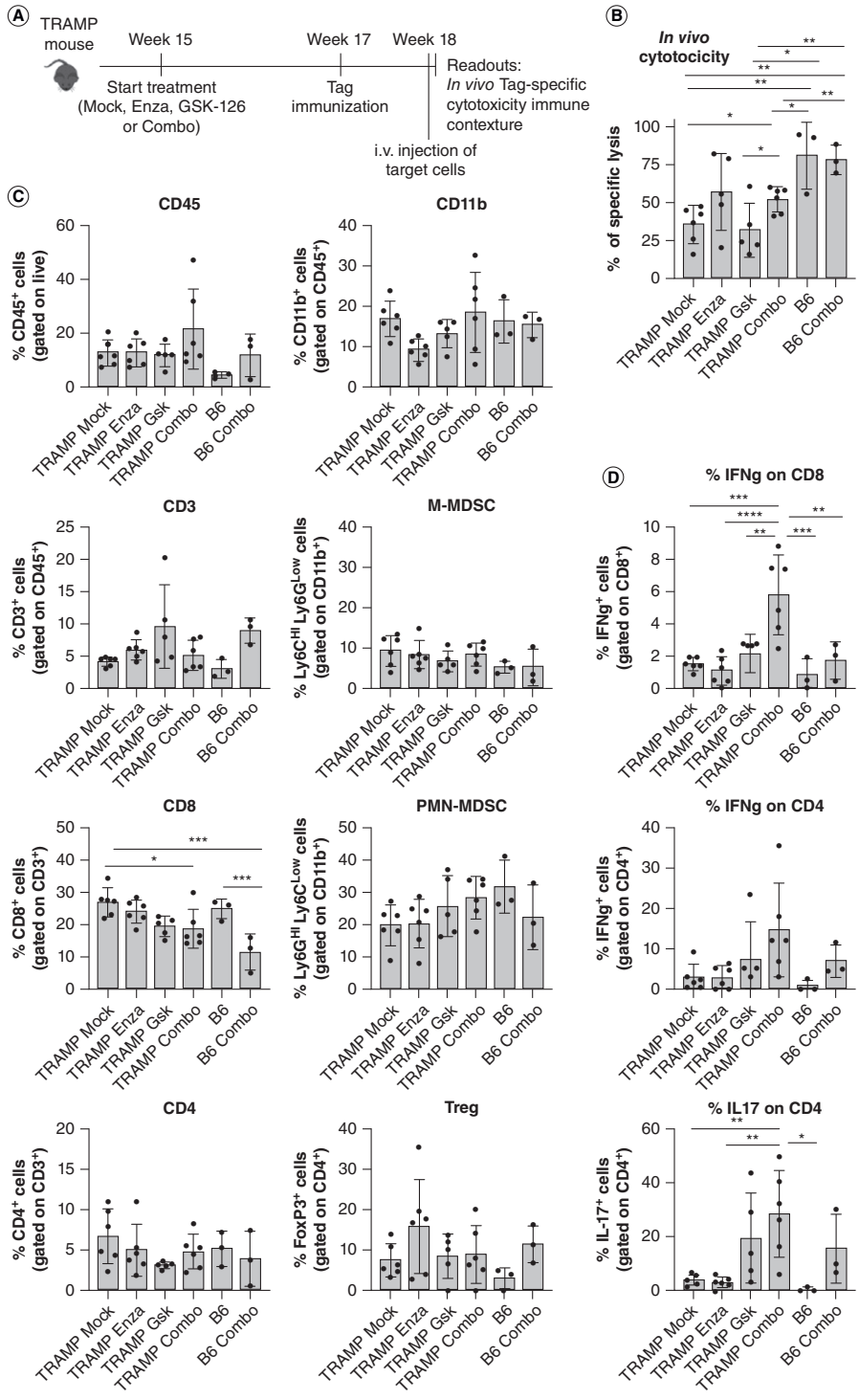

Figure 5. Concomitant inhibition of AR and EZH2 enhances cytotoxic activity and cytokine production of tumor-specific CD8$^+$ T cells. (A) Scheme of the *in vivo* cytotoxicity assay in TRAMP mice. 15-week-old TRAMP mice were treated with enzalutamide, GSK-126, or their combination (Combo). 2 weeks later treated TRAMP and control non-tumor-bearing naive C57BL/6 (B6) mice were immunized with DCs pulsed with Tag_{IV} peptide. 1 week later, *in vivo* cytotoxicity was tested as described in methods **(B)**. From these mice we also evaluated frequency **(C)** and cytokine production **(D)** of prostate-infiltrating immune cells, after 4 h stimulation with PMA-ionomycin and brefeldin A. Histograms report mean ± SD, each dot is a mouse. One-way ANOVA followed by Tukey's multiple comparison test: *$p < 0.05$; **$p < 0.01$; ***$p < 0.001$ and ****$p < 0.0001$. Where p-value is not indicated, the comparison between groups is not statistically significant.

Taylor & Francis
Taylor & Francis Group

The effect of the COMBO on T cell function depends on microenvironment

In vivo experiments indicate that the COMBO treatment can increase cytotoxicity and IFN-γ production of tumor-specific $CD8^+$ T cells (Figure 5). This could be either a direct effect or an indirect effect involving their crosstalk with other cells in the microenvironment. *In vitro* experiments excluded the first hypothesis, as no differences on proliferation and IFN-γ production were detected in purified $CD8^+$ or $CD4^+$ T cells treated *in vitro* with the COMBO (Figure 6A). As $CD4^+$ T cells in TRAMP prostates treated with COMBO produce more IL-17, we also tested such induction in either conventional T ($CD4^+$ $FoxP3^{neg}$) or Treg cells ($CD4^+$ $FoxP3^+$) treated *in vitro*, observing no significant changes (Figure 6B).

Having described that PMN-MDSC contribute to $CD8^+$ T cell tolerance in TRAMP mice [9], we also investigated the suppressive activity of PMN-MDSC isolated from TRAMP mice previously treated with enzalutamide, GSK-126 or the COMBO, finding no significant modulation (Figure 6C). As for M-MDSC, not suppressive in TRAMP mice [9], none of the treatments altered their functions (Figure 6C).

We also measured the production of $CD8^+$ T-cell stimulating cytokines, IFN-γ and IL-2 [50,51], by T1525, T23 and ST4787 tumor cells after *in vitro* treatment. Interestingly, the COMBO significantly increased the production of both IFN-γ and IL-2 in all tumor cells, albeit the former reached only very low levels (Supplementary Figure 6). However, the COMBO also seemed to enhance the release of IL-17, which can instead blunt Th1 activity [52]. This result suggests that, in tumor bearing mice treated with the COMBO, tumor cell could play a role in shaping T cell activation. This possible crosstalk would be the object of future investigation.

In conclusion, our results show that the simultaneous administration of enzalutamide and GSK-126 can restore tumor cell sensitivity to enzalutamide, reduce NEPC differentiation and simultaneously awake the anti-tumor specific T-cell response, *in vivo*, such to restrain the growth of prostate cancer. They also suggest that the increased T cell activity that we see *in vivo* as a consequence of the combination therapy could be related to the crosstalk with other cells in the microenvironment, including tumor cell themselves, however excluding MDSC as a relevant player in this setting.

Discussion

Effective treatment of CRPC and NEPC remains an unmet clinical need. Immune-checkpoint blockade revolutionized the therapy of many solid tumors, but proved scarce success in 'cold' prostate cancer. To identify new approaches for reverting castration resistance and simultaneously blunting immune suppression, we here investigated in preclinical models the combination of enzalutamide with the EZH2 inhibitor GSK-126.

In vitro, the COMBO treatment restored enzalutamide sensitivity in otherwise resistant cells, as similarly shown in other preclinical models [37,38]. Importantly, our results moved the finding further ahead proving the effectiveness of this combination *in vivo* against NEPC differentiation, and establishing the importance of the immune system to gain therapeutic efficacy of both enzalutamide alone and the COMBO. It is worth to say that in our *in vivo* experiments we used a relatively low dose of GSK-126 (30 mg/Kg) compared with that administered in other studies. Yet, we think that our results are not in contrast with the existing literature for several reasons. Indeed, we did not demonstrate any *in vivo* antitumor activity by GSK-126 when administered alone; rather, the effect was only observed when we combined GSK-126 and enzalutamide. Thus, our data do not contradict the findings from the paper of Huang *et al.* [25], which tested GSK-126 as a single agent (showing that only doses higher than 50 mg/Kg have antitumor activity). A different paper evaluated a single dose of GSK-126 in a completely different model (iv. injection of human tumor cells in nude mice, to model experimental metastases) [53]; therefore, it is difficult to make a comparison with our subcutaneous prostate cancer models. Lastly, as far as combination with either castration or enzalutamide was tested in immunodeficient mice [27,37], these were performed on prostate cancer models different from those used in our study. It is conceivable that different cells may have different sensitivity to GSK-126 doses. Alternatively, we could speculate that the relatively low dose of GSK-126 we administered might have unveiled the possibility to appreciate its direct effects on the microenvironment, which might have been otherwise masked by a strong direct activity on tumor cells exerted by higher doses of GSK-126. These results would require further investigation to determine the possible benefit of adding immunotherapy after enzalutamide and GSK-126 conditioning of the microenvironment. However, it is worth noting that both the manuscripts from Bolis and Ku [27,37] lack a comparison with a syngeneic, immunocompetent model.

Furthermore, the 30 mg/Kg dosage was also used in the paper by Peng *et al.* [21], which showed that the combination of GSK-126 and a second epigenetic modulator (the DNMT inhibitor 5-AZA-dC) synergized with adoptive T cell transfer, causing increased tumor T cell infiltration, production of Th1-type chemokines, and

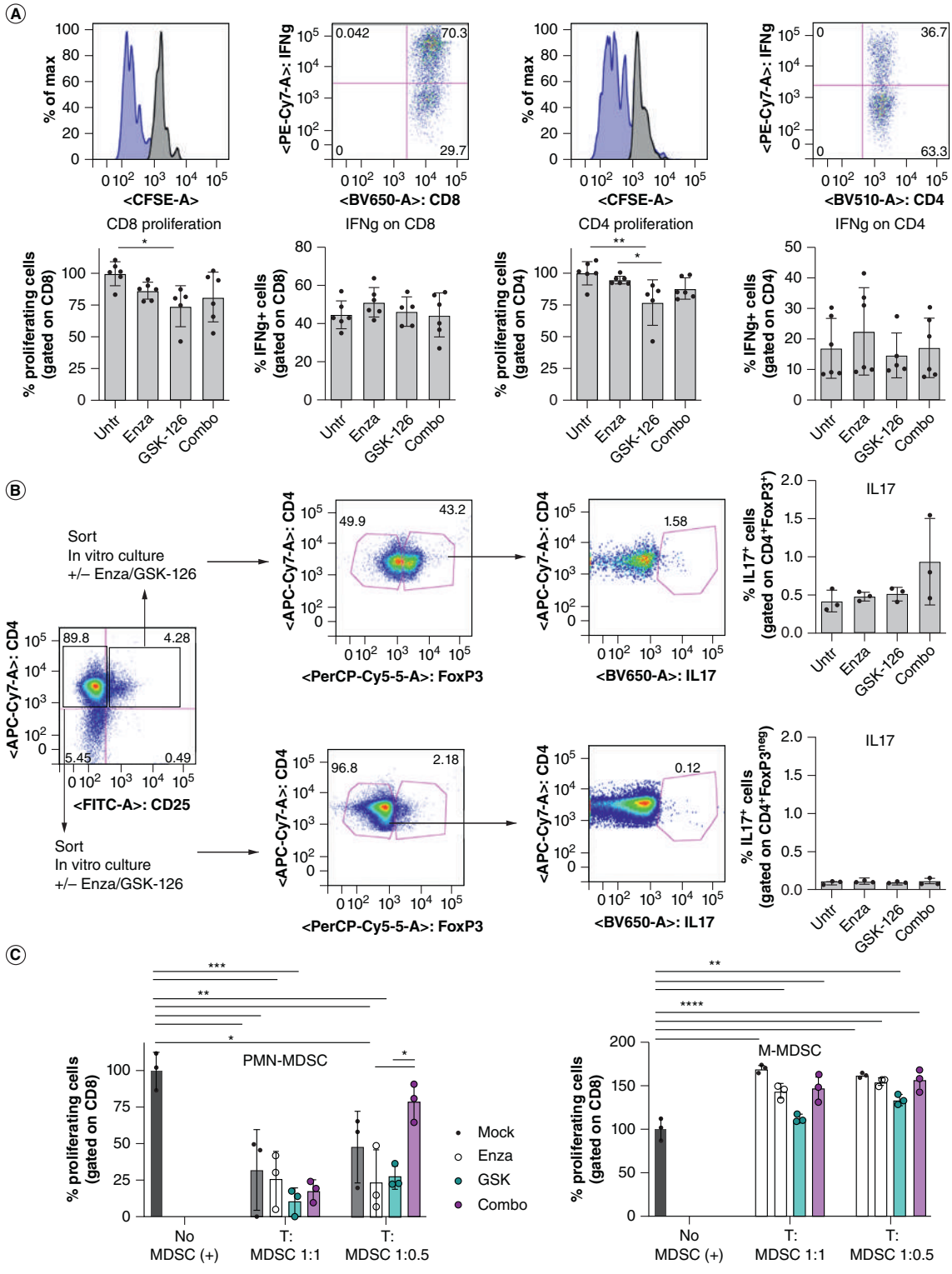

Figure 6. The COMBO treatment does not affect T cell and MDSC activity *in vitro*. (A) Naive T lymphocytes purified from the spleen of C57BL/6 mice were labeled with CFSE, activated *in vitro* with CD3/CD28 and treated with enzalutamide, GSK-126 or the Combo. 4 days later, proliferation (CFSE dilution) and IFN-γ production were evaluated by flow cytometry. **(B)** Flow cytometry evaluation of IL-17 production by T regulatory ($CD4^+CD25^+FoxP3^+$) or effector ($CD4^+CD25^{neg}FoxP3^{neg}$) T cells purified from tumor bearing mice and treated *in vitro* with enzalutamide, GSK-126 or combo. **(C)** PMN-MDSCs ($CD11b^+Ly6G^{hi}Ly6C^{int}$) and M-MDSC-like cells ($CD11b^+Ly6G^{low}Ly6C^{hi}$) isolated from TRAMP mice previously treated with enzalutamide, GSK-126 or the Combo were tested *in vitro* for suppressive activity against responder T cells. MDSC: responder ratio 1:1, 1:0.5 as indicated. All histograms report mean ± SD of biological replicates, represented by dots. One-way ANOVA followed by Tukey's multiple comparison test *$p < 0.05$; **$p < 0.01$; ***$p < 0.001$, and ****$p < 0.0001$. Where P-value is not indicated, the comparison between groups is not statistically significant.

reduction of tumor growth. Indeed, this and other papers showed that either EZH2 or AR inhibitors, alone, can trigger the production of inflammatory cytokines by $CD8^+$ and $CD4^+$ T cells in other tumor models [15,21,23]. Remarkably, while we observed that an intact immune system is needed to gain *in vivo* effectiveness of enzalutamide in a model that proved to be resistant *in vitro*, we found that only the enzalutamide and GSK-126 COMBO can awake tumor infiltrating T cells. Also, our observation that the two drugs did not systemically modulate immune cells, except for splenic macrophages, and did not directly alter T cell activity, suggests that an interplay with tumor cells and/or with other elements of the microenvironment is necessary to restore anti-tumor T cell function, *in vivo*. Nevertheless, our effort to identify the nature of such supporting cells has been so far elusive and will be object of future studies.

Differently from what shown in another NEPC model [37], in the ST4787 NEPC cell line GSK-126 administration did not restore sensitivity to enzalutamide. As NEPC emerges from CRPC in a lineage-plasticity process occurring through several intermediate states [2,4], it is conceivable that the DKO and TKO models used by Ku [37] and our ST4787 cell line represent different intermediates in this transition, with ST4787 closer to fully committed NEPC and no longer sensitive to epigenetic modulation. Nevertheless, as already shown *in vitro* [54], EZH2 inhibition can efficiently restrain NEPC differentiation induced *in vivo* by ADT/ARPI, underscoring that the COMBO should be initiated before completion of the CRPC-to-NEPC transition to be effective.

Furthermore, *in vivo*, the microenvironment of ST4787 NEPC tumors was infiltrated by low numbers of immune cells, and, among the few infiltrating, by a marked reduction of $CD8^+$ T cells and a strong increase in Treg cells, in comparison to T23-derived CRPC tumors. In such a 'cold' NEPC microenvironment, the potential benefic effect of the COMBO treatment on T cell activation would not be sufficient to overcome immunosuppression. These differences in the CRPC and NEPC immune milieu would require further investigation in additional prostate cancer models and in patient-derived specimens, such to establish the possible benefit of adding immunotherapy (i.e., immune-checkpoint blockade therapy) after enzalutamide and GSK-126 conditioning of the antitumor immune response. Further investigation is also required to dissect the alterations induced in the tumor microenvironment by either ADT or ARPI alone, as well as their combination. These analyses will be the focus of future research, building upon the findings presented in this paper.

Conclusion

We here provide evidence that the concomitant inhibition of AR and EZH2 can restrain CRPC growth and NEPC differentiation, restoring tumor cell sensitivity to enzalutamide, and also awakening anti-tumor T-cell response, opening new roads for immunotherapy in prostate cancer.

Summary points

- Castration-resistant prostate cancer (CRPC) is initially responsive to androgen receptor pathway inhibitors, like enzalutamide, but resistance eventually occurs, often associated to the emergence of aggressive neuroendocrine prostate cancer.
- Immunotherapy showed no efficacy in prostate cancer so far due to the immunosuppressive microenvironment.
- We tested a new therapeutic approach combining enzalutamide and GSK-126, an inhibitor of the epigenetic regulator EZH2 in both *in vitro* and *in vivo* models of prostate cancer.
- GSK-126 treatment confers enzalutamide sensitivity to otherwise resistant prostate cancer cells.
- GSK-126 and enzalutamide combination blocks CRPC growth and neuroendocrine prostate cancer differentiation in mouse models.
- Antitumor efficacy of GSK-126 and enzalutamide combination is lost in immunodeficient mice.
- GSK-126 and enzalutamide combination restore the activity of tumor-specific $CD8^+$ T cells in the TRAMP spontaneous model.
- These results promote future clinical investigation of the combined use of enzalutamide and GSK-126 against CRPC and neuroendocrine prostate cancer, also opening new possibilities for immunotherapy in prostate cancer.

Supplementary data

To view the supplementary data that accompany this paper please visit the journal website at: www.futuremedicine.com/doi/suppl/10.2217/epi-2023-0374

Author contributions

I Fischetti: investigation, methodology, writing-original draft, visualization. L Botti: investigation. R Sulsenti: investigation. V Cancila: investigation. C Enriquez: investigation. R Ferri: investigation, methodology. M Bregni: resources. F Crivelli: resources. C Tripodo: investigation, validation. MP Colombo: supervision, funding acquisition, writing reviewing and editing. E Jachetti: conceptualization, investigation, supervision, funding acquisition, writing-original draft, writing review and editing, visualization.

Acknowledgments

We thank Fondazione IRCCS Istituto Nazionale dei Tumori: Ester Grande for administrative assistance and Lorena Ventura for technical assistance with immunohistochemistry.

Financial disclosure

This work was supported by Grants from Fondazione IRCCS Istituto Nazionale dei Tumori, Milano (Bando per la Valorizzazione della Ricerca Istituzionale, BRI, 2018 to E.J.), Italian Ministry of Health (GR-2016-02362484 to E.J. and "Ricerca Corrente Funds") and Associazione Italiana per la Ricerca sul Cancro (AIRC; Investigator Grant 24363 to MPC). The authors have no other relevant affiliations or financial involvement with any organization or entity with a financial interest in or financial conflict with the subject matter or materials discussed in the manuscript apart from those disclosed.

Competing interest disclosure

The authors have no competing interests or relevant affiliations with any organization or entity with the subject matter or materials discussed in the manuscript. This includes employment, consultancies, honoraria, stock ownership or options, expert testimony, grants or patents received or pending, or royalties.

Writing disclosure

No writing assistance was utilized in the production of this manuscript.

Ethical conduct of research

Prostatectomies from prostate cancer patients were obtained from ASST Valle Olona, Busto Arsizio (VA), Italy (Protocol number 0046679/18), upon informed consent and in accordance with the Helsinki Declaration. Tissue collection, fixation and processing followed standardized protocols as part of routine clinical activity. Animal housing and experimentation were performed following institutional guidelines and the Italian law (D.Lgs. 26/2014). In vivo experiments were approved by the Italian Ministry of Health (authorization number 8/2020-PR).

Open access

This work is licensed under the Attribution-NonCommercial-NoDerivatives 4.0 Unported License. To view a copy of this license, visit http://creativecommons.org/licenses/by-nc-nd/4.0/

References

Papers of special note have been highlighted as: • of interest; •• of considerable interest

1. Sung H, Ferlay J, Siegel RL *et al.* Global Cancer Statistics 2020: GLOBOCAN Estimates of Incidence and Mortality Worldwide for 36 Cancers in 185 Countries. *CA Cancer J. Clin.* 71(3), 209–249 (2021).
2. Davies AH, Beltran H, Zoubeidi A. Cellular plasticity and the neuroendocrine phenotype in prostate cancer. *Nat. Rev. Urol.* 15(5), 271–286 (2018).
3. Aggarwal R, Huang J, Alumkal JJ *et al.* Clinical and genomic characterization of treatment-emergent small-cell neuroendocrine prostate cancer: a multi-institutional prospective study. *J. Clin. Oncol.* 36(24), 2492–2503 (2018).
4. Beltran H, Hruszkewycz A, Scher HI *et al.* The role of lineage plasticity in prostate cancer therapy resistance. *Clin. Cancer Res.* 25(23), 6916–6924 (2019).
5. Drake CG, Sharma P, Gerritsen W. Metastatic castration-resistant prostate cancer: new therapies, novel combination strategies and implications for immunotherapy. *Oncogene* 33(43), 5053–5064 (2014).
6. Bilusic M, Madan RA, Gulley JL. Immunotherapy of prostate cancer: facts and hopes. *Clin. Cancer Res.* 23(22), 6764–6770 (2017).
7. Drake CG. Prostate cancer as a model for tumour immunotherapy. *Nat. Rev. Immunol.* 10(8), 580–593 (2010).
8. Idorn M, Kollgaard T, Kongsted P, Sengelov L, Thor Straten P. Correlation between frequencies of blood monocytic myeloid-derived suppressor cells, regulatory T cells and negative prognostic markers in patients with castration-resistant metastatic prostate cancer. *Cancer Immunol. Immunother.* 63(11), 1177–1187 (2014).

9. Jachetti E, Cancila V, Rigoni A *et al.* Cross-Talk between myeloid-derived suppressor cells and mast cells mediates tumor-specific immunosuppression in prostate cancer. *Cancer Immunol. Res.* 6(5), 552–565 (2018).
10. Sorrentino C, Musiani P, Pompa P, Cipollone G, Di Carlo E. Androgen deprivation boosts prostatic infiltration of cytotoxic and regulatory T lymphocytes and has no effect on disease-free survival in prostate cancer patients. *Clin. Cancer Res.* 17(6), 1571–1581 (2011).
11. Calcinotto A, Spataro C, Zagato E *et al.* IL-23 secreted by myeloid cells drives castration-resistant prostate cancer. *Nature* 559(7714), 363–369 (2018).
12. Cioni B, Zwart W, Bergman AM. Androgen receptor moonlighting in the prostate cancer microenvironment. *Endocr. Relat. Cancer* 25(6), R331–R349 (2018).
13. Gubbels Bupp MR, Jorgensen TN. Androgen-induced immunosuppression. *Front. Immunol.* 9, 794 (2018).
14. Walecki M, Eisel F, Klug J *et al.* Androgen receptor modulates Foxp3 expression in $CD4^+CD25^+Foxp3^+$ regulatory T-cells. *Mol. Biol. Cell* 26(15), 2845–2857 (2015).

• **Preclinical study showing that androgen receptor (AR) can control FoxP3 expression in Tregs.**

15. Guan X, Polesso F, Wang C *et al.* Androgen receptor activity in T cells limits checkpoint blockade efficacy. *Nature* 606(7915), 791–796 (2022).

•• **Seminal paper showing that AR can directly prevent the expression of IFN-γ and granzyme B in CD8 T cells, thus blunting T cell activation.**

16. Becerra-Diaz M, Strickland AB, Keselman A, Heller NM. Androgen and androgen receptor as enhancers of M2 macrophage polarization in allergic lung inflammation. *J. Immunol.* 201(10), 2923–2933 (2018).
17. Scalerandi MV, Peinetti N, Leimgruber C *et al.* Inefficient N2-like neutrophils are promoted by androgens during infection. *Front. Immunol.* 9, 1980 (2018).
18. Trigunaite A, Khan A, Der E, Song A, Varikuti S, Jorgensen TN. Gr-1(high) $CD11b^+$ cells suppress B cell differentiation and lupus-like disease in lupus-prone male mice. *Arthritis Rheum.* 65(9), 2392–2402 (2013).
19. Consiglio CR, Udartseva O, Ramsey KD, Bush C, Gollnick SO. Enzalutamide, an androgen receptor antagonist, enhances myeloid cell-mediated immune suppression and tumor progression. *Cancer Immunol. Res.* 8(9), 1215–1227 (2020).

• **This work in mouse models shows that enzalutamide enhances myeloid-derived suppressor cells recruitment and favors the growth of AR-negative tumors.**

20. Vire E, Brenner C, Deplus R *et al.* The polycomb group protein EZH2 directly controls DNA methylation. *Nature* 439(7078), 871–874 (2006).
21. Peng D, Kryczek I, Nagarsheth N *et al.* Epigenetic silencing of TH1-type chemokines shapes tumour immunity and immunotherapy. *Nature* 527(7577), 249–253 (2015).

•• **First paper demonstrating that the inhibition of EZH2 enhances T cell activation and response to anti-PD-1 immunotherapy.**

22. Wang D, Quiros J, Mahuron K *et al.* Targeting EZH2 reprograms intratumoral regulatory T cells to enhance cancer immunity. *Cell Rep.* 23(11), 3262–3274 (2018).
23. Goswami S, Apostolou I, Zhang J *et al.* Modulation of EZH2 expression in T cells improves efficacy of anti-CTLA-4 therapy. *J. Clin. Invest.* 128(9), 3813–3818 (2018).

• **Paper confirming that EZH2 inhibition stimulates T cell function and improves the effectiveness of anti-CTLA-4 immunotherapy in mouse models.**

24. Zhou J, Liu M, Sun H *et al.* Hepatoma-intrinsic CCRK inhibition diminishes myeloid-derived suppressor cell immunosuppression and enhances immune-checkpoint blockade efficacy. *Gut* 67(5), 931–944 (2018).
25. Huang S, Wang Z, Zhou J *et al.* EZH2 Inhibitor GSK126 suppresses antitumor immunity by driving production of myeloid-derived suppressor cells. *Cancer Res.* 79(8), 2009–2020 (2019).
26. Li C, Song J, Guo Z *et al.* EZH2 inhibitors suppress colorectal cancer by regulating macrophage polarization in the tumor microenvironment. *Front. Immunol.* 13, 857808 (2022).
27. Bolis M, Bossi D, Vallerga A *et al.* Dynamic prostate cancer transcriptome analysis delineates the trajectory to disease progression. *Nat. Commun.* 12(1), 7033 (2021).
28. Yamagishi M, Uchimaru K. Targeting EZH2 in cancer therapy. *Curr. Opin. Oncol.* 29(5), 375–381 (2017).
29. Kim KH, Roberts CW. Targeting EZH2 in cancer. *Nat. Med.* 22(2), 128–134 (2016).
30. Varambally S, Dhanasekaran SM, Zhou M *et al.* The polycomb group protein EZH2 is involved in progression of prostate cancer. *Nature* 419(6907), 624–629 (2002).
31. Cao Q, Yu J, Dhanasekaran SM *et al.* Repression of E-cadherin by the polycomb group protein EZH2 in cancer. *Oncogene* 27(58), 7274–7284 (2008).
32. Yu J, Yu J, Rhodes DR *et al.* A polycomb repression signature in metastatic prostate cancer predicts cancer outcome. *Cancer Res.* 67(22), 10657–10663 (2007).

33. Liu Q, Wang G, Li Q *et al.* Polycomb group proteins EZH2 and EED directly regulate androgen receptor in advanced prostate cancer. *Int. J. Cancer* 145(2), 415–426 (2019).
34. Kim J, Lee Y, Lu X *et al.* Polycomb- and methylation-independent roles of EZH2 as a transcription activator. *Cell Rep.* 25(10), 2808–2820; e2804 (2018).
35. Xu K, Wu ZJ, Groner AC *et al.* EZH2 oncogenic activity in castration-resistant prostate cancer cells is polycomb-independent. *Science* 338(6113), 1465–1469 (2012).
36. Dardenne E, Beltran H, Benelli M *et al.* N-Myc induces an EZH2-mediated transcriptional program driving neuroendocrine prostate cancer. *Cancer Cell* 30(4), 563–577 (2016).

• **Elegant demonstration in mouse models that EZH2 mediates neuroendocrine prostate cancer development.**

37. Ku SY, Rosario S, Wang Y *et al.* Rb1 and Trp53 cooperate to suppress prostate cancer lineage plasticity, metastasis, and antiandrogen resistance. *Science* 355(6320), 78–83 (2017).

•• **First demonstration in the PBCre4:Pten$^{fl/fl}$:Rb1$^{fl/fl}$:Trp53$^{fl/fl}$ mouse model that EZH2 inhibition restores sensitivity to enzalutamide.**

38. Xiao L, Tien JC, Vo J *et al.* Epigenetic reprogramming with antisense oligonucleotides enhances the effectiveness of androgen receptor inhibition in castration-resistant prostate cancer. *Cancer Res.* 78(20), 5731–5740 (2018).
39. Pittoni P, Tripodo C, Piconese S *et al.* Mast cell targeting hampers prostate adenocarcinoma development but promotes the occurrence of highly malignant neuroendocrine cancers. *Cancer Res.* 71(18), 5987–5997 (2011).
40. Sulsenti RFB, Bongiovanni L, Cancila V *et al.* Repurposing of the Antiepileptic Drug Levetiracetam to Restrain Neuroendocrine Prostate Cancer and Inhibit Mast Cell Support to Adenocarcinoma. *Front. Immunol.* 12, 622001 (2021).
41. Greenberg NM, Demayo F, Finegold MJ *et al.* Prostate cancer in a transgenic mouse. *Proc. Natl Acad Sci. USA* 92(8), 3439–3443 (1995).
42. Enriquez C, Cancila V, Ferri R *et al.* Castration-induced down-regulation of SPARC in stromal cells drives neuroendocrine differentiation of prostate cancer. *Cancer Res.* 81(16), 4257–4274 (2021).
43. Beltran H, Tomlins S, Aparicio A *et al.* Aggressive variants of castration-resistant prostate cancer. *Clin. Cancer Res.* 20(11), 2846–2850 (2014).
44. Li Y, Chan SC, Brand LJ, Hwang TH, Silverstein KA, Dehm SM. Androgen receptor splice variants mediate enzalutamide resistance in castration-resistant prostate cancer cell lines. *Cancer Res.* 73(2), 483–489 (2013).
45. Smith R, Liu M, Liby T *et al.* Enzalutamide response in a panel of prostate cancer cell lines reveals a role for glucocorticoid receptor in enzalutamide resistant disease. *Sci. Rep.* 10(1), 21750 (2020).
46. Masoodi KZ, Eisermann K, Yang Z *et al.* Inhibition of androgen receptor function and level in castration-resistant prostate cancer cells by 2-[(isoxazol-4-ylmethyl)thio]-1-(4-phenylpiperazin-1-yl)ethanone. *Endocrinology* 158(10), 3152–3161 (2017).
47. Ishikawa F, Yasukawa M, Lyons B *et al.* Development of functional human blood and immune systems in NOD/SCID/IL2 receptor gamma chain(null) mice. *Blood* 106(5), 1565–1573 (2005).
48. Degl'innocenti E, Grioni M, Boni A *et al.* Peripheral T cell tolerance occurs early during spontaneous prostate cancer development and can be rescued by dendritic cell immunization. *Eur. J. Immunol.* 35(1), 66–75 (2005).
49. Mylin LM, Bonneau RH, Lippolis JD, Tevethia SS. Hierarchy among multiple H-2b-restricted cytotoxic T-lymphocyte epitopes within simian virus 40 T antigen. *J. Virol.* 69(11), 6665–6677 (1995).
50. Bhat P, Leggatt G, Waterhouse N, Frazer IH. Interferon-gamma derived from cytotoxic lymphocytes directly enhances their motility and cytotoxicity. *Cell Death Dis.* 8(6), e2836 (2017).
51. Ross SH, Cantrell DA. Signaling and function of interleukin-2 in T lymphocytes. *Annu. Rev. Immunol.* 36, 411–433 (2018).
52. Mills KHG. IL-17 and IL-17-producing cells in protection versus pathology. *Nat. Rev. Immunol.* 23(1), 38–54 (2023).
53. Chen YT, Zhu F, Lin WR, Ying RB, Yang YP, Zeng LH. The novel EZH2 inhibitor, GSK126, suppresses cell migration and angiogenesis via down-regulating VEGF-A. *Cancer Chemother. Pharmacol.* 77(4), 757–765 (2016).
54. Puca L, Bareja R, Prandi D *et al.* Patient derived organoids to model rare prostate cancer phenotypes. *Nat. Commun.* 9(1), 2404 (2018).

Taylor & Francis
Taylor & Francis Group